Journal of Theoretical and Applied Information Technology
10th February 2013. Vol. 48 No.1

ISSN: 1992-8645 www.jatit.org E-ISSN: 1817-3195

MODELING AND MICRO SCALE ANALYZING OF MICRO-SWITCH APPLIED IN ALL-OPTICAL COMMUNICATION

[1]TIAN WENCHAO, [2]CHEN ZHIQIANG
[1, 2]School of Electro-Mechanical Engineering, Xidian University, Xi'an, 710071, China
E-mail: tianwenchao@21cn.com

ABSTRACT

Inductive micro-switch is an integrative device of a sensor and actuator and widely applied in all-optical-network communication. Its malfunctions related to "fail-to-closure" and "transient-closure" result in low reliability and weak anti-jamming capability. A new bistable inductive micro-switch is presented based on micro electro-mechanical system (MEMS) technology. A sine rough surface model is used to describe the random distribution of the rough adhesive surface. Micro size Casimir and van der Waals (vdW) forces are analyzed in detail. The vdW force includes the repulsive force. Dynamic simulation results are shown to be in agreement with experimental results. The threshold acceleration was 6.8g, and the response time was 17.5μs. A "double-snap-back" phenomenon in the Off-state is discovered.

Keywords: *Inductive Micro-Switch; Casimir Force; Van Der Waals Force; Double-Snap-Back*

1. INTRODUCTION

Micro-switch is a key device in all-optical-net communication and widely applied Optical Layer Cross Connect (OLXC). Based on the MEMS technology, an inductive micro-switch can not only induce an external acceleration, but can also be controlled by the external acceleration to realize the optical trigger action. When the external acceleration is less than the threshold acceleration, the micro-switch maintains its Off-state. When the external acceleration reaches the threshold value, the micro-switch is triggered quickly to realize its On-state automatically, and an external circuit is switched on.

The inductive micro-switch is an integrative device consisting of a sensor and actuator. It is small, simple, low-cost, highly sensitive and fast responsive. Based on these characteristics, the inductive micro-switch is applied widely in the triggering field, such as in the automotive air restraint system, space probe callback system, fairing firing separation system, crashworthy data protection system of portable computer etc. Zhao et al design a micro-switch with a post-bucking structure for the airbag restraint system [1]. However, their micro-switch beam is too fragile making it too difficult to assemble. Alexander et al design a dual-mass-spring micro-switch [2], which used an inductive mass to induct the external acceleration. That design has a "fail-to-closure" problem such that before the external acceleration reaches the threshold acceleration, the inductive mass could strike the fixed electrode inducing a premature On-state. Therefore, the system's reliability is very low. Yang et al design a snake-shape beam micro-switch [3]. In that design when the external acceleration reaches the threshold acceleration, an inductive mass strikes the fixed electrode to realize the trigger action. But the elastic force pulls the inductive mass quickly back to the Off-state. Therefore, this micro-switch can not realize a stable contact, and the external circuit can not maintain a stable On-state. It clearly has a problem of "transient-closure". Du et al analyze the plastic deformation in the micro-switch contact area [4]. Esquivel analyzes the Casimir force in the micro-switch [5]. Ongkodjojo et al design a micro switch for health care applications [6]. However, the micro switch can not precisely and reliably control the external circuit to switch.

Little work has been done to develop a comprehensive model to accurately analyze the micro size force during the micro-switch contact process. Therefore, current inductive micro-switches lack stability in the Off-state or On-state, and can not trigger accurately at the threshold acceleration. Malfunction of the existing inductive micro-switch, i.e., "fail-to-closure" and "transient-closure", results in low reliability and weak anti-jamming capability.

In this paper, we present an inductive micro-switch with a bistable structure based on the adhesive effect. A sine-model is used to describe the rough contact surface of the micro-switch.

Journal of Theoretical and Applied Information Technology
10th February 2013. Vol. 48 No.1

ISSN: 1992-8645 www.jatit.org E-ISSN: 1817-3195

Micro size forces such as the Casimir force and van der Waals (vdW) force are analyzed. In the Off-state, a "double-snap-back" phenomenon is discovered. It is shown that the designed micro-switch can be accurately controlled to realize the trigger action. Due to the bistable structure, the micro-switch has strong antijamming capability and high reliability. The dynamic simulation results indicate the threshold acceleration is 6.8g, and the response time is 17.5μs.

2. INDUCTIVE MICRO SWITCH WITH BISTABLE STRUCTURE

Figure 1 shows a silicon inductive micro-switch with a bistable structure. Both of the lower surfaces of the inertial mass, 4, and the upper surface of the bottom cover, 3, are deposited by gold to form electrodes and connect with an external circuit. Fe is the electrostatic force between the moveable electrode, 6, and the fixed electrode, 8, and Fk is the elastic force of beam, 5. Fc and Ff are the Casimir force and vdW force between the mass, 4, and the top cover, 1, respectively. Since the tip, 6, and fixed electrode, 8, do not contact the mode shown in Figure 1 is in an Off-state.

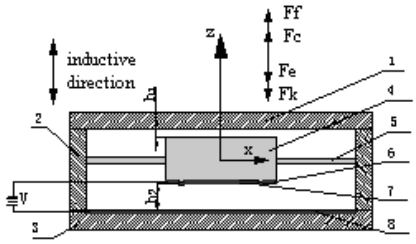

Figure1. Inductive Switch With Bistable Structure In Off-State (1: Top Cover 2: Side Frame 3: Bottom Cover 4: Mass Block 5: Support Beam 6: Moveable Electrode 7: Contact Tip 8: Fixed Electrode)

In the Off-state, the distance, h1, is less than 1μm. F_f and F_c are micro size forces. According to the micro size effect, F_f and F_c lead the mass, 4, to adhere to the top cover, 1. This is the first stable state, realized when the external acceleration is less than the threshold acceleration, i.e., $F_c + F_f > F_e + F_k + F_m$. Here, F_m is the inertia force caused by the external acceleration. Micro size forces, Fc and Ff, can ensure that the mass block, 4, does not to move down to avoid "fail-on-closure" malfunction.

When the external acceleration reaches the threshold acceleration, i.e., $F_c + F_f < F_e + F_k + F_m$, the mass block, 4, moves down and strikes at the bottom cover, 3, quickly, bringing the tip, 7, in contact with the fixed electrode, 8. In that case, the micro-switch is in the On-state, and the external circuit switches on. This is another stable state. The distance between the moveable electrode, 6, and fixed electrode, 8, is less than 1μm. According to the micro size effect, F_c and F_f exist between the moveable electrode, 6, and the fixed electrode, 8, which can ensure that the mass block, 4, closely adheres to the bottom cover, 3. Even if there is an external interferential acceleration, ad, the mass block, 4, remains in a stable contact model and can not be separated from the bottom cover, 3. This stable contact practically avoids the "transient-closure" malfunction.

3. CASIMIR FORCE F_C

Philip Ball [7] discovers that vacuum energy appears in the form of particles that forms or disappears ceaselessly in the form of particulates. Generally, the vacuum is filled with particulates with various wave lengths. Long waves are excluded, but other waves induce an attraction, which makes two thin slices stay closely attached to each other. The attraction is inverse proportion to the gap between the slices, i.e., the closer the slices, the greater the attraction. This effect is called the Casimir effect, and the attraction is known as the Casimir force. According to the theory of the vacuum energy [8], the Casimir force for two smooth parallel plates is:

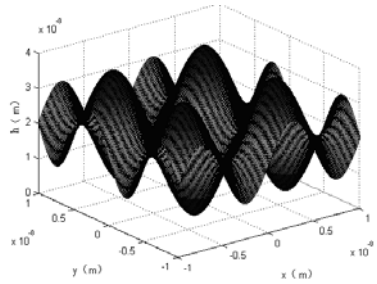

Figure2. Sine Model Of Rough Surface

$$F_0 = \frac{-\varepsilon \hbar c \pi^2}{240 h^4} \quad (1)$$

ε is the dielectric constant, $\hbar$ the reduced Planck's constant, c the speed of light, h the gap. A micro-switch is typically manufactured by the microfabrication technology, such as lithography, etching, deposition, bonding and so on. Surfaces of the mass block, 4, the top cover, 1, and electrodes 6, 8 shown in Figure1, although may be considered smooth in a macroscopic scale, are rough in the microscopic scale. According to Hariri's result [9], contact between two rough surfaces can be

Journal of Theoretical and Applied Information Technology
10th February 2013. Vol. 48 No.1

ISSN: 1992-8645 www.jatit.org E-ISSN: 1817-3195

simulated with a smooth-rough contact model. As shown in Figure1, we assume that the inner surface of the top cover, 1, is smooth, and the top surface of the mass block, 4, is rough. We have modeled this rough surface by the following sine distribution (also shown in Figure2):

$$h(x,y) = A\left[\sin(\frac{2\pi x}{T}) + \sin(\frac{2\pi y}{T})\right] \quad (2)$$

A=10nm is the amplitude of this rough surface, and T=10nm is the peak-valley density cycle. The Casimir force between the top cover, 1, and the mass block, 4, in Off-state is described by equation (3), where L=3mm, D=1mm are the length and width of the mass block, 4, respectively.

$$F_c = \frac{1}{LD}\int_{-L/2}^{L/2}\int_{-D/2}^{D/2}\frac{-\varepsilon\hbar c\pi^2}{240 z_h^{\,4}}dxdy$$
$$= \frac{-\varepsilon\hbar c\pi^2}{240}\left(\frac{1}{z_h^{\,4}} + \frac{3.12A^2}{z_h^{\,6}}\right. \quad (3)$$
$$\left. + \frac{1.36A^3}{z_h^{\,7}} + \frac{10.95A^4}{z_h^{\,8}}\right)$$

In the Off-state, zh is given by:

$$z_h = z - h_1 - h(x,y) \quad (4)$$

While in the On-state, zh is given by:

$$z_h = h_2 + h(x,y) - z \quad (5)$$

z is the vertical displacement of mass block 4 in Figure1. h1=0.1μm, h2=7μm and h(x,y) is described by equation (2).

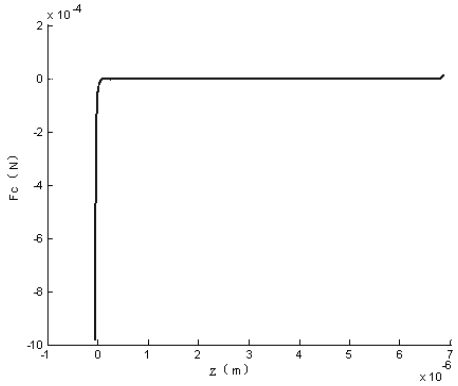

Figure3. Relationship Between Fc And Z

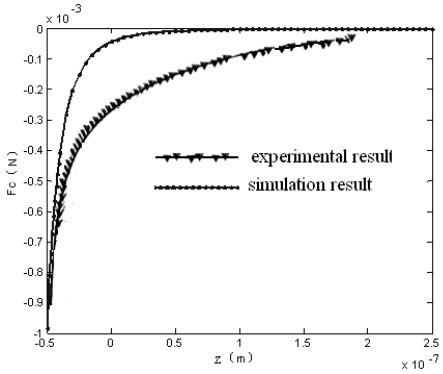

Figure4. Partial Enlargement Of Figure3 In Off-State Along With Experimental Result [10]

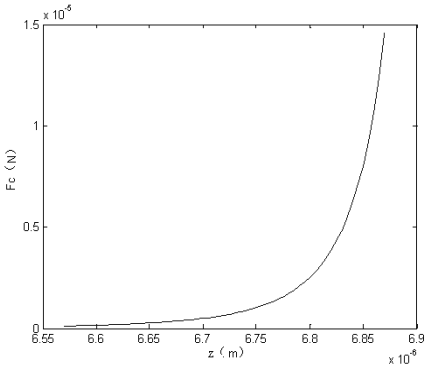

Figure5. Partial Enlargement Of Fig 3 In On-State

The integral result of equation (3) is very complicated. So it is omitted here.

The simulation result is shown in Figure3. As shown in Figure3, We can see that the Casimir force is nearly zero when gaps are big enough. As gaps decrease, the Casimir force becomes big. This is known as the micro size effect. Figure4 is a partial enlargement of Figure3 along with an experimental result [10] in the Off-state. The simulation result is shown to be in agreement with the experimental result. The Casimir force is produced by the gap between the top cover, 1, and the mass block, 4. Figure 5 is a partial enlargement of Figure3 in the On-state. The Casimir force is produced by the gap between the electrodes, 6 and 8.

4. VAN DER WAALS FORCE F_f

Dipole effects of moment orientation, induction and dispersion in the micro structure result in a dispersion force, London force and Debye force. The sum of these forces is known as the vdW force. The Lennar-Jones potential describes the double-atom vdW force.

Journal of Theoretical and Applied Information Technology
10th February 2013. Vol. 48 No.1

ISSN: 1992-8645 www.jatit.org E-ISSN: 1817-3195

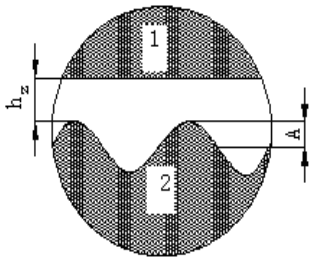

Figure6 Van Der Waals Force Model

Figure6 shows the vdW force model of the micro switch shown in Figure1 in the Off-state. Part 1 represents the inner surface of the top cover, 1, Part 2 the top surface of the mass block, 4. Small circles represent the atoms. The interactions between two atoms are given by the Lennar-Jones potential.

Reference [11] analyzes Hamaker three hypotheses and discovers that there is contradiction between the continuous medium hypotheses and constant material properties hypotheses. Reference [12] presents a Wigner-Seitz micro continuum medium principle which is further verified in Reference [13]. According to the Wigner-Seitz micro continuum medium principle, the vdW force shown in Figure 3 is given by:

$$F_f = \frac{\pi^2 \rho^2_{w-s} B_1}{180 \lambda_1 z_h^{\ 8}} - \frac{\pi^2 \rho^2_{w-s} B_2}{6 \lambda_2 z_h^{\ 2}} \qquad (14)$$

Similarly, in the micro-switch On-state, the van der Waals force can be described by

$$F_f = \frac{\pi^2 \rho^2_{w-s} B_1}{180 \lambda_1 z_h^{\ 8}} - \frac{\pi^2 \rho^2_{w-s} B_2}{6 \lambda_2 z_h^{\ 2}} \qquad (15)$$

where zh is described by Eq. (5).

5. DYNAMIC ANALYSES

The dynamic of the micro-switch is described by the following force balance over the inertial mass:

$$m\ddot{z} + \xi \dot{z} + kz = \begin{cases} F_e - F_c - F_f + ma & \text{Off-state} \\ F_e + F_c + F_f + ma & \text{On-state} \end{cases} \qquad (16)$$

With the acceleration, a, given by $a = 100t$. In Eq. (16), ξ is the air damping coefficient between electrodes, 6, and 8; $k = \frac{EL_3 L_2^{\ 3}}{4L_1^{\ 3}}$ is the elasticity coefficient; E is the elastic modulus of the support beam, 5; L1, L2 and L3 are the length, width and height of the beam, 5, respectively; m the mass, 4; $F_e = \frac{\varepsilon LDU^2}{Z_h^{\ 2}}$ is the electrostatic force. ε is the dielectric constant; L and D are the length and width of the mass, 4, and U the voltage between electrodes, 6, and 8. Table 1 lists the simulation parameters used in the present modeling.

Table 1 Simulation Parameters

m(mg)	6.99
E(Gpa)	120
ξ(mN.s/m)	0.05
L_1(mm)	3
L_2(mm)	0.1
L_3(mm)	0.1
U(V)	30
ε(F/m)	8.854×10-12
L （mm）	3
D(mm)	1

The simulation results are shown in Figure 7, 8, 9 and 10. Figs.8 and 9 are partial enlargements of Figure7. Figure10 is a partial enlargement of Figure9. Figure7 shows the displacement variation with time. Figure8 shows the “double-snap-back” in the Off-state at t=0.01ms and t=0.028ms, which is agreed with Ref.[13] It is shown that even when an interfering acceleration exists, the micro size force ensures that the mass does not strike downward, thus avoiding the “fail-to-closure” malfunction. The micro switch has high anti-jamming capability. Figure 9 shows that the micro-switch is triggered at t=0.67ms. The threshold acceleration is 67m/s2 (=6.8g where g is an acceleration of gravity). The response time is 17.5μs. Figure10 shows that there is a snap-back point at t=0.6868ms, which ensures the mass to adhere closely the bottom cover, thus avoiding the “transient-closure” malfunction. The micro switch has high reliability.

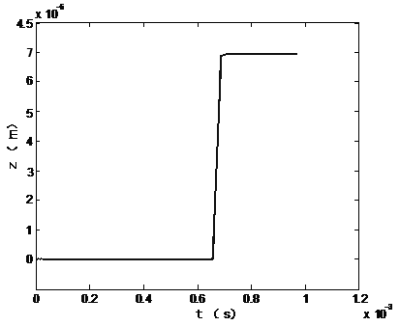

Figure7. Simulation Result Of Displacement

ISSN: 1992-8645 www.jatit.org E-ISSN: 1817-3195

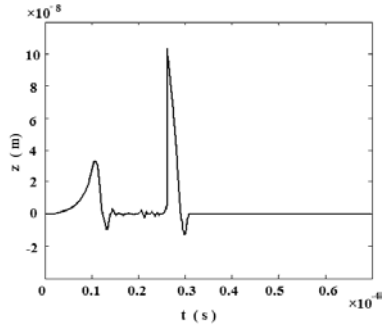

Figure8. Snap Back In Off-State

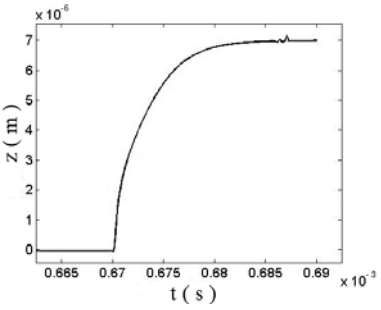

Figure9. Partial Enlargement Of Figure4 In Trigger Process

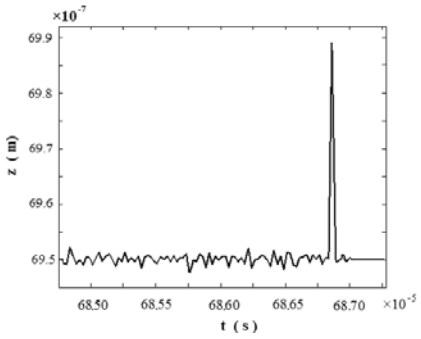

Figure10. Snap Back In On-State

6. CONCLUSIONS

At the typical malfunctions of "fail-to-closure" and "transient-closure" in the current inductive micro-switch are addressed here by a new design of a bistable inductive micro-switch based on the micro size force. The switch performance is simulated by describing the adhesive rough surface by a sine shape. The micro size forces of the Casimir force and van der Waals forces are analyzed. The simulation results of the Casimir force varied with the gap are obtained, which is compared with the relative experimental result. The dynamic equation of the bistable inductive micro switch is established. The simulation results of the displacement varied time are obtained. It is shown that in the Off-state, the micro-switch has "double-snap-back" and two inflection points. In the On-state, the micro-switch has "single-snap-back", which is agreed with relative reference. Dynamic simulation results are presented for a threshold acceleration of 6.8g, response time of 17.5μs. Under these conditions the micro switch is shown to have a high anti-jamming capability.

ACKNOWLEDGMENT

This work supported by Research Program supported by the National Natural Science Foundation of China (61176130).

REFRENCES:

[1] Zhao, J., Jia J., He, X. and Wang, H.， Post-buckling and snap-through behavior of inclined slender beams, Journal of Applied Mechanics, 75(7) (2008) 041020-041026.

[2] Alexander, R. N., Werner, F. R. and Martin H., Influence of electrical and mechanical parameters on contact welding in low power switches，IEEE Transactions on Components and Packaging Technology, 27(1)(2004) 4-11.

[3] Yang, Z., Ding, G., Cai, H., Liu, R. and Zhao X.,， A novel design and fabrication of MEMS electrical inertia micro–switch, China mechanical engineering, 19(9)(2008)1132-1136.

[4] Du, Y., Chen L., McGruer, N. E., Adams, G. G. and Etsion I., A finite element model of loading and unloading of an asperity contact with adhesion and plasticity, Journal of Colloid and Interface Science, 312(2)(2007)522-528.

[5] Esquivel, S. R., Pull-in control in micros-witches using acoustic Casimir forces, Europhysics Letters, 84(2008) 48002-48007.

[6] Ongkodjojo, A. and Francis, E., Optimized design of a micro-machined g-switch based on contactless configuration for health care applications, Journal of Physics: Conference Series, 34(2006)1044-1052, Singapore.

[7] Ball, P., Feel the force, Nature, 447（2007） 772-774.

[8] Munday, J. N., Capasso F. and Parsegian V. A., Measured long-range repulsive Casimir–Lifshitz forces, Nature, 457(2009)170-173.

[9] Hariri, A., Zu, J. W. and Mrad, R. B., Modeling of dry stiction in micro electro-mechanical systems (MEMS)， Journal of Micromechanics and Microengineering, 16(7)(2006)1195-1206.

ISSN: 1992-8645 www.jatit.org E-ISSN: 1817-3195

[10] Hertlein, C., Helden, L., Gambass, A., Dietrich, S. and Bechinger, C., Direct measurement of critical Casimir force, Nature, 451(2008)172-175.

[11] Tian, W. and Jia J., Analysis of Hamaker continuum mediun hypothesis, Acta Physica Sinica, 57(9) (2008)5378-5383.

[12] Tian, W. and Jia J., Micro Continuum Analysis of Wigner-Seitz Model, Acta Physica Sinica, 58(9) (2009)5930-5935.

[13] Tian W., Wang L. and Jia J., Casimir force, Hamaker force, Stiction and snap-back, Acta Physica Sinica, 59(2) (2010)1175-1179.